

Did stress triggering cause the large off-fault aftershocks of the 25 March 1998 $M_w=8.1$ Antarctic plate earthquake?

Shinji Toda

Central Research Institute of Electric Power Industry, Japan
toda@criepi.denken.or.jp

Ross S. Stein

U. S. Geological Survey, Menlo Park
rstein@usgs.gov

Abstract. The 1998 Antarctic plate earthquake produced clusters of aftershocks ($M_w \leq 6.4$) up to 80 km from the fault rupture and up to 100 km beyond the end of the rupture. Because the mainshock occurred far from the nearest plate boundary and the nearest recorded earthquake, it is unusually isolated from the stress perturbations caused by other earthquakes, making it a good candidate for stress transfer analysis despite the absence of near-field observations. We thus tested five proposed source models for the main rupture. We find that for 4 of the 5 models, 64-93% of the off-fault aftershocks lie in regions brought closer to Coulomb failure by the main rupture, typically by 1-2 bars (0.1-0.2 MPa). The Antarctic plate event, together with the 1992 $M_w = 7.3$ Landers and its $M_w = 6.5$ Big Bear aftershock 40 km from the main fault, supply evidence that small stress changes can indeed trigger large earthquakes far from the main fault rupture.

Introduction

The 25 March 1998 $M_w=8.1$ Antarctic plate earthquake is one of the largest oceanic strike-slip events ever recorded. In addition to its spectacular size, the earthquake has two unique characteristics that motivate our study. The first is that the mainshock

occurred about 250 km from the nearest plate boundary (Fig. 1), and 100 km from the nearest earthquake (a $M_w=5.6$ event in 1981) recorded by the Harvard CMT and ISC catalogs since their inception in 1966 and 1976, respectively. The presumed left-lateral fault is also at a high angle to the left-lateral transform boundary (Fig. 1), suggesting that the stress driving the Antarctic plate fault is not a product of plate boundary motion. For these reasons, the site of the 1998 shock is likely to be unusually isolated from the stress transfer from large nearby earthquakes.

The other remarkable attribute of the Antarctic plate event is that its aftershocks are distributed over an extent of 350 km, with the largest $M_w=6.4$ event striking 100 km from of the mainshock and 80 km south of the inferred fault rupture (Fig. 1). Such large distant aftershocks or coupled mainshocks are not unknown. The 1812 $M_w\sim 7.5$ Wrightwood, California, earthquake on the San Andreas fault was followed 13 days later by the $M_w\sim 7.1$ Santa Barbara shock 200 km away; *Deng and Sykes* [1996] argued that the second shock was brought closer to Coulomb failure by the first. Most recently, the 1992 $M_w = 7.3$ Landers earthquake was followed 3.5 hrs later by the $M_w=6.5$ Big Bear shock 40 km away. *King et al.* [1994] argued that the Big Bear shock was promoted by the stress changes associated with the Landers rupture. In many respects, the Antarctic plate event appears to be a larger version of the Landers-Big Bear sequence.

The absence of near-field observations of the Antarctic plate earthquake, however, adds uncertainty to any conclusions one can draw about the stress transfer. Although the earthquake is well studied using teleseismic waveforms, yielding source parameters, slip functions, and aftershock locations, there are 15-25 km uncertainties in the location of the fault rupture, and 5 km uncertainties in the location of the aftershocks with respect to the mainshock [*Nettles et al.*, 1999; *Antolik et al.*, 1998]. Thus, given its unique attributes tempered by its limitations, we seek to use the Antarctic plate event to learn whether distant large aftershocks can be triggered or promoted by the stress transferred

from the main rupture. Here we find that the presence of the remote southern and western aftershocks can be explained by the calculated Coulomb failure stress increases.

Methods and Assumptions

We calculate the static Coulomb failure stress change, which is expressed as $\Delta\sigma_f = \Delta\tau - \mu\Delta\sigma$, where $\Delta\tau$ is the shear stress change resolved on a given failure plane (reckoned positive in the direction of fault slip), $\Delta\sigma$ is the normal stress change (positive in compression) and μ is the coefficient of friction. Positive values of the Coulomb stress change are interpreted to promote failure, negative values to inhibit failure. We compute stress changes in an elastic halfspace [Okada, 1992] with a shear modulus of 3.2×10^{10} Nm⁻² and a Poisson's ratio of 0.25. See King *et al.* [1994], Harris *et al.* [1995], and Harris [1998] for discussion about the method.

For the Antarctic plate earthquake, we consider source models of McGuire *et al.* [1998], Nettles *et al.* [1999], Henry and Das [1999], and Antolik *et al.* [1999]. The faults are shown in Fig. 1, and slip functions in Fig. 2. All models have been constrained by their authors to pass through the NEIC epicenter, which has a ~15-km location uncertainty, and all show a concentration of slip near the CMT epicenter (Figure 2). Nettles *et al.* [1999] found two main subevents separated by 125 km, the first subevent having twice the moment of the second, so we also consider the possibility that the second subevent was triggered by static stress transfer from the first, 60 sec later.

While the rupture length is determined in each source model by waveform inversion, the fault width (its down-dip dimension) is poorly constrained. The width is crucial to our study, however, because the fault length-to-width ratio controls the intensity of the stress-change lobes off the slipped fault. A long rupture relative to its width, such as the Great 1906 San Francisco earthquake, profoundly drops the stress athwart or off the fault, whereas a short fault produces intense off-fault lobes in which

failure is promoted [King *et al.*, 1994]. Here we set the fault width of all but the *Antolik et al.* [1999] model to 30 km, for the following reasons. The oceanic crust is 35-55 my old at the site of the Antarctic plate earthquake, [Müller *et al.*, 1997]. Such an age yields a 27-38 km depth of the 700-800° isotherm [Parsons and Sclater, 1977], which *Wiens and Stein* [1983, 1984] found corresponds to the thickness of the seismogenic lithosphere. If, on the other hand, the fault width were less than 15-20 km, the slip would be unrealistically high for its moment. *Wells and Coppersmith* [1994], for example, report 11 m as the peak observed slip in $M_w=8$ continental strike-slip events, whereas a width of 15 km would yield a mean slip of 25 m for the Antarctic event. We calculate the stress changes at a depth of 15 km, half the fault width, although our sensitivity tests indicate that the stress patterns are largely unchanged at depths of 5-25 km.

To assess the spatial association between aftershocks and the calculated static stress changes, we use the locations of the five largest aftershocks from the Harvard CMT catalog, as well as the locations of 17 $m_b \geq 3.7$ aftershocks from *Nettles et al.* [1999] using JHD relocations with residuals less than 3.5 sec; and 31 $m_b \geq 3.9$ events from *Antolik et al.* [1999] using a 3D harmonic earth model. Since we are focused on the stress transfer to the site of off-fault shocks, we resolve the Coulomb stress changes on vertical, left-lateral faults striking 275°, the average strike of the left-lateral nodal plane of the mainshock and the five largest aftershocks (Fig. 1).

Results

Calculated Coulomb stress changes are sensitive to the assumed friction coefficient. Friction controls the distribution of the Coulomb stress change off the fault. As μ increases, the off-fault lobes grow in size and shift into the dilatant quadrants, where faults are unclamped. We have set $\mu = 0.8$ because a high value of friction fits the aftershocks distribution best. Friction of 0.8 is consistent with laboratory experiments for

dry rock samples [Byerlee, 1978]. In a stress-transfer study, *Parsons et al.* [1999] found that $\mu \geq 0.8$ for faults that lacked significant cumulative slip, which is likely true for the Antarctic plate fault. In the presence of high fluid pressures or extensive fault gouge, however, μ could be as low as 0.0-0.2, in which case the southern aftershocks could not be explained as a consequence of static stress transfer.

Simple models of the Antarctic plate earthquake are consistent with the off-fault shocks being brought closer to failure. *McGuire et al.* [1998] inverted for the first and second central moments of the moment-rate distribution in space and time, constrained by the Harvard CMT solution. We explored a range of locations for the source fault consistent with the 25 km uncertainty relative to the NEIC epicenter given by *McGuire et al.* When the fault is shifted 25 km to the east, 93% of the *Nettles et al.* aftershocks and 79% of the *Antolik et al.* aftershocks located ≥ 20 km from the rupture lie in regions brought closer to failure (Fig. 3a). Some 87-94% of the aftershocks lie in regions brought closer to failure by the first subevent of *Nettles et al.* [1999] (Fig. 3b). In addition, the rupture surface of the second subevent in *Nettles et al.* is brought 0.5-2.0 bars (0.05-0.20 MPa) closer to failure by rupture of the first subevent, (for this calculation, we resolved the stress changes on the 270° strike of the second subevent).

More detailed slip functions yield more diverse results, in which two models fit the aftershock distribution well, and one does not. When we consider both subevents of *Nettles et al.* [1999], 55-64% of the aftershocks lie in regions where stress is calculated to have increased (Fig. 3c). The 360-km-long variable slip model of *Henry and Das* [1999] produces the broadest stress shadow, although it displays western and southern off-fault zones similar to that of *McGuire et al.* [1998]. Some 53-67% of aftershocks lie in regions brought closer to failure; if the *Henry and Das* source is shifted 18 km to the east, within the 25-km location uncertainty, 76-85% of the aftershocks lie in regions brought closer to failure (Fig. 3d). Because of its more heterogeneous slip distribution (Fig. 2), the *Antolik et al.* [1999] model produces numerous off-fault lobes (Fig. 3e). In this model,

faulting extends through the western aftershock cluster, and the southern cluster lies in the stress shadow. Thus, none of the off-fault aftershocks lie in regions brought closer to failure, regardless of the nodal plane used to resolve the stress changes.

Discussion and Conclusions

For all but the *Antolik et al.* model, 60-94% of the off-fault aftershocks lie in regions calculated to have been brought closer to failure. This percentage rises to 85-93% when two models are shifted 18-25 km eastward. Such a displacement is within the relative location error of the source models (Fig. 1). The aftershock-stress association is, however, predicated on the assignment of a 30-km fault width and the assumption of a high coefficient of friction, which we can not independently verify. We therefore evaluated the significance of the aftershock-stress correlations with the equal-tails test of the null hypothesis that the association is random, taking into account the degrees of freedom inherent in our modeling (setting the friction coefficient, width, and for some correlations, shifting the location of the source). In seven cases, the correlations are significant at the $\geq 99\%$ confidence level; these include the *McGuire et al.* model when shifted 25 km east (Fig. 3a); the *Nettles et al.* first subevent (Fig. 3b), the *Nettles et al.* two-subevent model when shifted 18 km west; and the *Henry and Das* model when shifted 18 km east (Fig. 3d). All but one of these correlations is significant when using either the *Nettles et al.* or *Antolik et al.* aftershocks. Three correlations are significant at the $>95\%$ level [*McGuire et al.*, unshifted; both subevents of *Nettles et al.*, unshifted (Fig. 3c); *Henry and Das*, unshifted], and five are not significant ($<95\%$). Thus, most of the tested Antarctic plate source models are consistent with off-fault and fault-end shocks being triggered by stress increases of more than 1-2-bars (0.1-0.2 MPa).

In contrast to the off-fault shocks, aftershocks along the source faults, or within 20 km of the model faults, are generally inconsistent with the areas of calculated

Coulomb stress increase. This may be because the detailed pattern of slip is poorly resolved, and thus the stress changes close to the fault are unknown. Further, we calculated the stress changes on vertical, left-lateral planes striking 275° . If some of the aftershocks near the fault occur on secondary faults with different orientations, the calculated stress change would be different. Another feature common to all the models is that there are few aftershocks in the northern off-fault lobe or the eastern fault-end lobe (Fig. 3). We speculate that the secular stresses buildup at the transform plate boundary (Fig. 1) may inhibit failure to the northeast of the Antarctic plate shock.

In summary, the extraordinary distribution of aftershocks of the Antarctic plate event may indeed be a product of static stress transfer. The Antarctic plate and Landers-Big Bear sequences together suggest that the seismic hazard posed by large aftershocks off the main fault can be assessed by stress-transfer calculations. In both the California and Antarctic events, aftershocks struck in regions brought 1-2 bars (0.1-0.2 MPa), and the time lags between mainshock and the largest aftershocks are short, 9.0 and 3.5 hours, respectively. The implications of such large and distant aftershocks for great San Andreas ruptures are provocative: A great earthquake on the southern San Andreas fault might, for example, trigger a large aftershock on the urban Newport-Inglewood fault, potentially causing more damage than the mainshock.

Acknowledgements. We thank Meredith Nettles for encouraging us to undertake this study; M. Antolik, S. Das, G. Ekström, C. Henry, J. McGuire, M. Nettles, and T. Wallace, for generously allowing us to use their unpublished preliminary source models; and R. Harris and T. Parsons for thoughtful and incisive reviews of the manuscript. We are also grateful to *Pacific Gas & Electric Co.* for funding this research.

References

- Antolik M., A. Kaverina, D. Dreger, and G. Ekström, Finite fault rupture models of the 25 March, 1998 (Mw=8.2) Balleny Sea earthquake, *EOS Trans., AGU, 1998 Fall Mtg.*, 79 (45), suppl., F662, 1998. [to be replaced by a ms. submitted to *Geophys. Res. Lett.*, 1999].
- Byerlee, J.D., Friction of rocks, *Pure Applied Geophys.*, 116, 615-626, 1978.
- Deng J., and L. R. Sykes, Triggering of 1812 Santa Barbara earthquake by a great San Andreas shock: Implications for future seismic hazards in southern California, *Geophys. Res. Lett.*, 23, 115-1158, 1996.
- Harris, R. A., Introduction to special section: Stress triggers, shadows, and implications for seismic hazard, *J. Geophys. Res.*, 103, 24,347-24,358, 1998.
- Harris, R. A., R. W. Simpson, and P. A. Reasenber, Influence of static stress changes on earthquake locations in southern California, *Nature*, 375, 221-224, 1995.
- Henry C., and S. Das, Rupture history of the 25th March, 1998, Balleny Islands earthquake, *EOS Trans., AGU, 1998 Fall Mtg.*, 79 (45), suppl., F662, 1998 [to be replaced by a ms. submitted to *Geophys. Res. Lett.*, 1999].
- King G. C. P., R. S. Stein, and J. Lin, Static stress changes and the triggering of earthquakes, *Bull. Seismol. Soc. Am.*, 84, 935-953, 1994.
- Nettles M., T. C. Wallace, and S. Beck, The March 25, 1998 Antarctic plate earthquake, in press, *Geophys. Res. Lett.*, 1999.
- Okada, Y., Internal deformation due to shear and tensile faults in a half space, *Bull. Seismol. Soc. Am.*, 82, 1018-1040, 1992.
- McGuire, J. J., L. Zhao, and T. H. Jordan, GSDF inversion for higher moments of the stress glut rate tensor, *EOS Trans., AGU, 1998 Fall Mtg.*, 79 (45), suppl., F658, 1998. [to be replaced by a ms. submitted to *Geophys. Res. Lett.*, 1999].
- Müller, R. D., W. R. Roest, J.-Y. Royer, L. M. Gagagan, and J. G. Sclater, Digital isochrons of the world's ocean floor, *J. Geophys. Res.*, 102, 3211-3214, 1997.

- Parsons, B., and J. G., An analysis of the variation of ocean floor bathymetry and heat flow with age, *J. Geophys. Res.*, **82**, 803-827, 1977.
- Parsons, T., R. S. Stein, R. W. Simpson, and P. A. Reasenber, Stress sensitivity of fault seismicity: A comparison between limited-offset oblique and major strike-slip faults, *J. Geophys. Res.*, in press, 1999.
- Stein R. S., G. C. P. King, and J. Lin, Stress triggering of the 1994 M=6.7 Northridge, California, earthquake by its predecessors, *Science*, **265**, 1432-1435, 1994.
- Wells, D. L., and K. J. Coppersmith, New empirical relationships among magnitude, rupture length, rupture width, rupture area, and surface displacement, *Bull. Seismol. Soc. Am.*, **84**, 974-1002, 1994.
- Wiens, D. A., and S. Stein, Age dependence of oceanic intraplate seismicity and implications for lithospheric evolution, *J. Geophys. Res.*, **88**, 6455-6468, 1983
- Wiens, D. A., and S. Stein, Intraplate seismicity and stresses in young oceanic lithosphere, *J. Geophys. Res.*, **89**, 11,442-11,464, 1984.

Figure Captions

Figure 1. Map of the 1998 Antarctic plate mainshock and largest relocated aftershocks ($m_b \geq 3.7$). The rift-transform boundary of the Antarctic and Australian plates is visible in the northeast corner of the map. The rupture planes for the five tested models, in the positions given by their authors, are depicted by the bold lines.

Figure 2. Slip functions for the rupture planes shown in Fig. 1, with the dip and rake indicated for each model. The width for all but the *Antolik et al.* model is set to 30 km.

Figure 3. Calculated static stress change for the five source models. The percentage of CMT and either *Nettles et al.* or *Antolik et al.* relocated aftershocks falling in regions of Coulomb stress increase is also shown. Only aftershocks more than 20 km from the model fault plane (outside of the white box) are counted; thus the total number of shocks differs for each model. The *McGuire et al.* and *Henry and Das* models are shown shifted east by the amounts indicated.

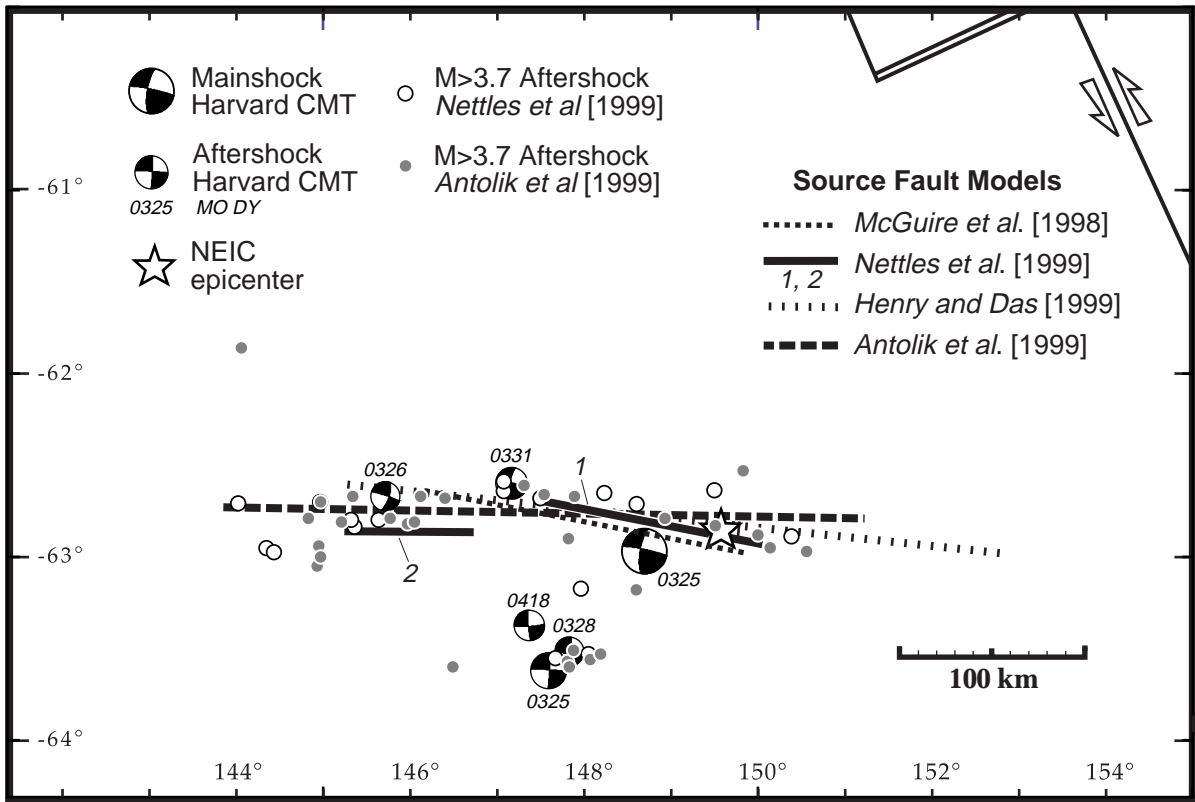


Figure 1 Toda and Stein (3/19/99)

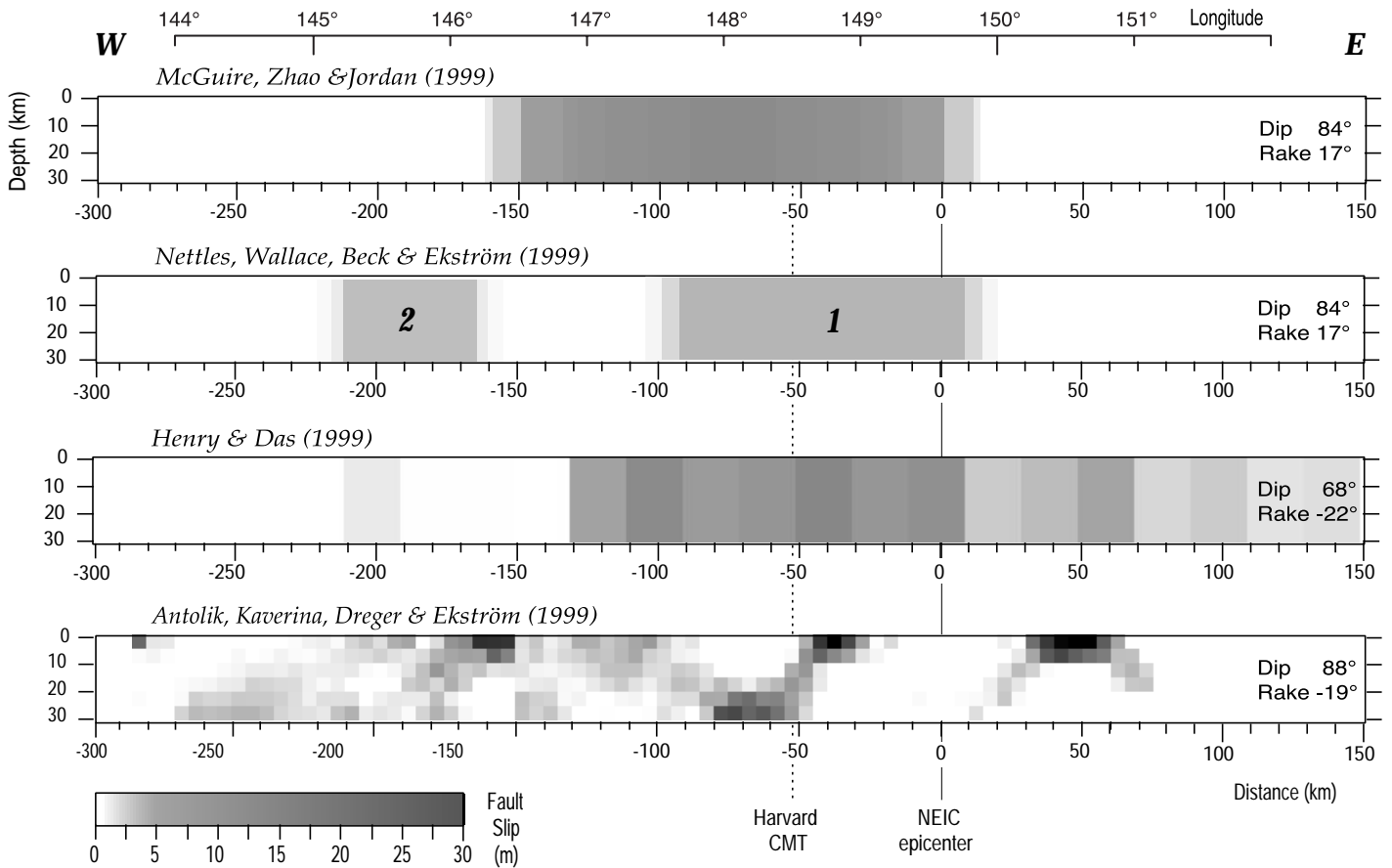


Figure 2 Toda and Stein (3/19/99)

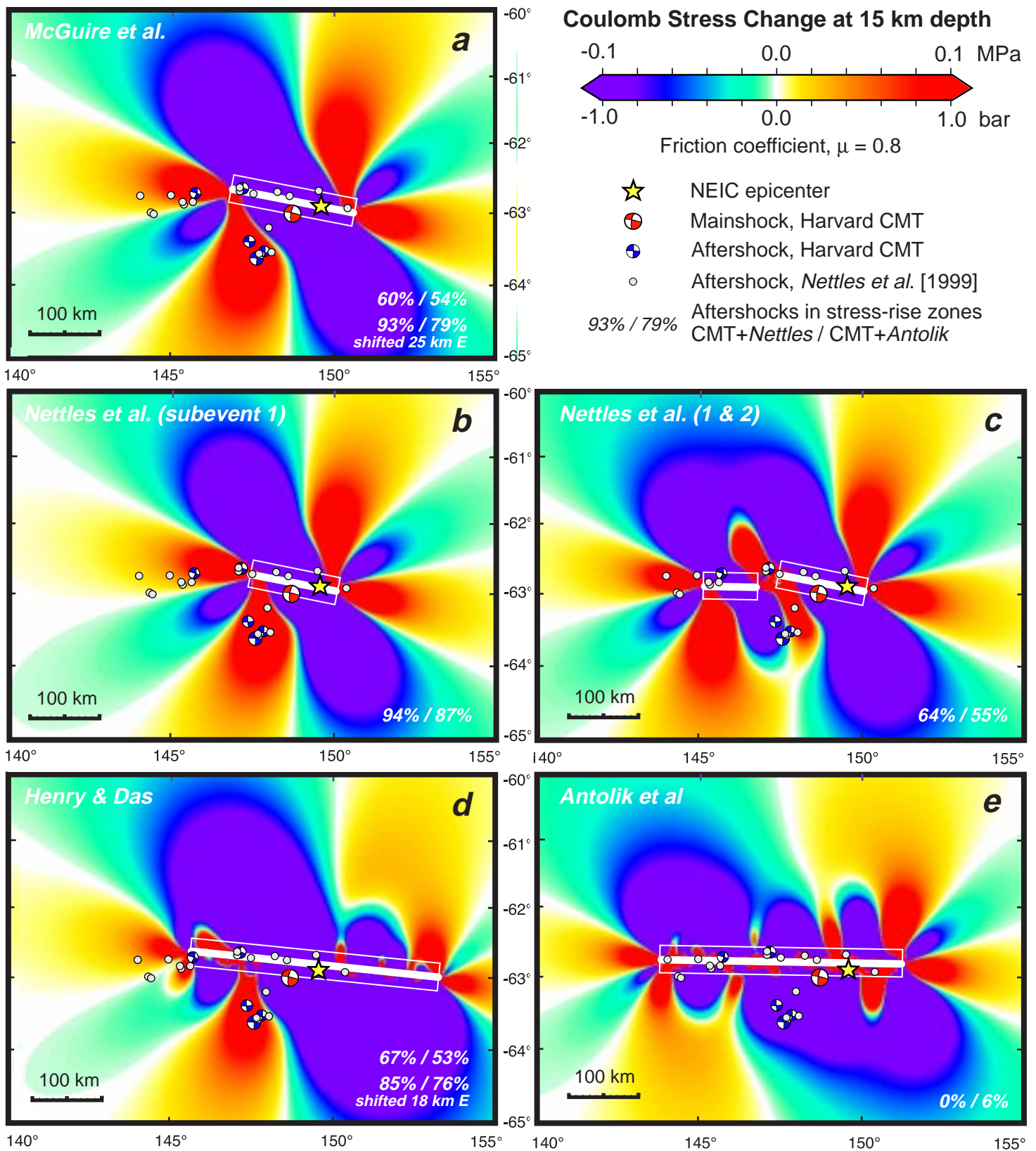


Figure 3 Toda and Stein (3/19/99)